

The Source of Maser Emission W33C (G 12.8–0.2)

P. Colom¹, E. E. Lekht², M. I. Pashchenko²,

and G. M. Rudnitskij²

¹*LESIA, Observatoire de Paris, Section de Meudon, 5 place Jules Janssen, Meudon, 92195 France*

²*M. V. Lomonosov Moscow State University, Sternberg Astronomical Institute, 13 Universitetskij prospekt, Moscow, 119234 Russia*
e-mail: lekht@sai.msu.ru

Abstract

Results of observations of the maser sources toward the W33C region (G12.8-0.2) carried out on the 22-m radio telescope of the Pushchino Radio Astronomy Observatory in the 1.35-cm H₂O line and on the Large radio telescope in Nançay (France) in the main (1665 and 1667 MHz) and satellite (1612 and 1720 MHz) OH lines are reported. Multiple, strongly variable short-lived H₂O emission features were detected in a broad interval of radial velocities, from –7 to 55 km/s. OH maser emission in the 1667-MHz line was discovered in a velocity range of 35–41 km/s. Stokes parameters of maser emission in the main OH lines 1665 and 1667 MHz were measured. Zeeman splitting was detected in the 1665-MHz line at 33.4 and 39.4 km/s and in the 1667 MHz line only at 39.4 km/s. The magnetic field intensity was estimated. A appreciable variability of Zeeman splitting components was observed at 39 and 39.8 km/s in both main lines. The extended spectrum and fast variability of the H₂O maser emission together with the variability of the Zeeman splitting components in the main OH lines can be due to the composite clumpy structure of the molecular cloud and to the presence in it of large-scale rotation and bipolar outflow as well as of turbulent motions of material.

The maser radio emission in the OH lines toward the HII region in the source W33C (G12.8–0.2) was detected by Pashchenko in 1975 [1, 2], and in the 1.35-cm water vapor line by Genzel and Downes in 1976 [3].

In this region the radio continuum source has two emission peaks. Observations at 408 MHz [4] and 5000 MHz [5] showed that the faintest component, G12.7–0.2, has a size of 5' × 4', while the size of the intense component, G12.8–0.2, is only 0.8'. The kinematic distance to G12.8–0.2 was estimated from the neutral-hydrogen absorption line profile as 5 kpc [6].

In January 1975 and October 1978 we carried out observations toward the continuum source W33C on the Large radio telescope in Nançay (France) in all four 18-cm OH lines, in both circular polarizations [1, 2]. Strongly polarized maser emission at velocities of 32.5 and 34.5 km/s on the background of strong absorption toward the HII region G12.8–0.2 was detected in the main 1665-MHz OH line. In the 1667-MHz line we observed faint emission, also on the background of strong absorption. We also determined the coordinates of the OH emission source: $\alpha_{1950} = 18^{\text{h}}11^{\text{m}}18.5^{\text{s}}$,

$\delta_{1950} = -17^{\circ}56' \pm 1.5'$. The OH maser is embedded in a compact molecular cloud, which is a source of type IIc OH emission in the 1612- and 1720-MHz satellite lines.

Subsequently, we conducted observations of the OH maser W33C in 1991 and 2008–2011. Unfortunately, in the literature there is no information about observations of this OH maser by other authors, either on single antennas or on high angular resolution systems. It should be noted that the W33 region hosts two centers of the 1665-MHz maser emission arranged symmetrically at both sides from W33C.

In November 1976 Genzel and Downes [3] detected on the 100-m radio telescope in Effelsberg intense H₂O maser emission of the source W33C at a wavelength of 1.35 cm in an interval of radial velocities from -4 to 1 km/s (8 Jy) and weaker emission (less than 4 Jy) at velocities from 30 to 41 km/s. The coordinates of the detected source to within measurement errors coincided with those of the OH maser source. Later, the H₂O maser W33C was observed by Jaffe et al. [7] and Comoretto et al. [8]. In 1981 the emission was notably weaker and took place at -7 and 34 km/s.

1 OBSERVATIONS AND DATA

The observations of the 1.35-cm H₂O maser radio emission in a line 1.35 cm toward the source W33C ($\alpha_{1950} = 18^{\text{h}}11^{\text{m}}18.3^{\text{s}}$, $\delta_{1950} = -17^{\circ}56'21''$) were carried out on the 22-m RT-22 radio telescope (Pushchino) in November 1981, and then since March 2010 to November 2011. The noise temperature of the system with a cooled frontend FET amplifier in the observations of this source was 120–270 K depending on weather conditions.

The signal analysis was implemented by a 2048-channel autocorrelator with a spectral resolution of 6.1 kHz (0.0822 km/s at 22 GHz). For a pointlike source an antenna temperature of 1 K corresponds to a flux density of 25 Jy [9].

The observations of the radio source W33C in the 18-cm hydroxyl lines were conducted on the radio telescope of the Nançay Radio Astronomy Station of the Paris–Meudon Observatory (France) at different epochs. The telescope is a Kraus system two-mirror instrument making possible observations of radio sources near the meridian. Using a spherical mirror allows us, by moving the feed, to track a radio source within $\pm 30^{\text{m}}/\cos\delta$ in the hour angle with respect to the meridian. At declination $\delta = 0^{\circ}$ the telescope beamwidth at a wavelength of 18 cm is $3.5' \times 19'$ in the right ascension and declination, respectively. The telescope sensitivity at $\lambda = 18$ cm and $\delta = 0^{\circ}$ is 1.4 K/Jy. The noise temperature of the helium-cooled amplifiers is from 35 to 60 K, depending on conditions of the observation.

The spectral analysis was conducted by an autocorrelation spectrum analyzer, the frequency resolution was 763 Hz. In the 1665- and 1667-MHz lines this corresponds to a radial-velocity resolution of 0.137 km/s. In the observations of 2010–2011 the resolution was twice as high, 0.068 km/s. Since 2008 the radio telescope simultaneously receives two perpendicular modes of linear polarization, which yield directly the intensities of the corresponding linear modes (L 0°, L 90°). Mixing signals from the perpendicular feeds with a phase delay of one of the modes by a quarter of the wavelength produces two orthogonal circular modes (LC, RC). Thus, three Stokes parameters I , V , and

Q are in fact observed simultaneously (with an appropriate choice of the coordinate system).

The observations were processed by the GILDAS software package of the Institute of Millimeter Radio Astronomy (IRAM, Grenoble, France), available on the Web at <http://www.iram.fr/IRAMFR/GILDAS/> [9].

Figure 1 presents the H₂O spectra for different epochs. A double-pointed arrow shows the scale in janskys. The horizontal axis is the velocity with respect to the Local Standard of Rest. Vertical bars at the bottom mark the velocities at which emission features were ever observed either by us or by other authors [3, 7, 8].

The H₂O maser emission was mostly observed in two spectral intervals: from -7 to $+1$ km/s and from 32 to 37 km/s (Fig. 2). Single emission features scattered in the spectrum from 9 to 55 km/s were also observed. Thus, the full velocity interval is about 62 km/s.

The results of our observations of the hydroxyl maser emission in the 1665- and 1667-MHz lines at different epochs are shown in Fig. 3. In 1975 and 1978 the observations were carried out with a resolution of 1 km/s, in 2008 with a resolution of 0.137 km/s, and in 2010–2011 with a resolution of 0.068 km/s. Solid curves show emission in the left-hand and dashed ones in the right-hand circular polarizations. The technique of the observations is described in [10, 11].

The results of the observations in the satellite lines (1612 and 1720 MHz) are shown in Fig. 4.

For the main lines 1665 and 1667 MHz Figures 5 and 6 show Stokes parameters for the epochs of December 5, 2008, and May 3, 2011, respectively. Time variations of Stokes parameter V for the central part of the 1665-MHz spectrum are presented in Fig. 7, and for the 1667-MHz line in Fig. 8. The main components are numbered, and their parameters are listed in Tables 1 and 2, where F_1, F_2, F_3, F_4 are flux densities of the components, $\delta V_{2,1}$ and $\delta V_{4,3}$ are velocity differences between components 2 and 1 and components 4 and 3, respectively.

2 DISCUSSION OF THE RESULTS

Though the maser emission source W33C was discovered long ago, it has been poorly studied either in the water-vapor line or in the hydroxyl lines. High angular resolution observations lack, and this does not allow us to spatially localize the observed emission features. Therefore, in the data analysis we concentrate on the variability of the maser emission.

2.1 H₂O Maser Emission

In spite of the fact that regular observations of the H₂O maser emission in G12.8–0.2 were conducted by us only since the beginning of 2010, we managed to find a number of important peculiarities of this emission. Let us list the main ones.

1. The emission spectrum is rather broad, from -7 to 55 km/s.
2. Most emission features are short-lived.

3. There are two groups of persistent emission features with a difference in radial velocities of ~ 37 km/s; the mean velocity of the second group (34 km/s) coincides with the central velocity of the OH absorption line and with the velocity of the OH maser emission.

4. There is a weak emission at 24 km/s, which was clearly visible after averaging the H₂O spectra (Fig. 2). This suggests this emission is faint but rather stable.

In addition to the H₂O spectrum, we have also detected a continuum signal with $T_a \sim 0.5$ K, which corresponds to a flux density of ~ 15 Jy.

2.2 Hydroxyl Emission

In all OH main-line profiles we observe strong absorption, on which the maser emission is superimposed. The absorption line with a central velocity of 35.8 km/s arises in a compact molecular cloud, which is also a source type IIc OH emission in the 1612- and 1720 MHz lines [2]. The absorption linewidth at half-maximum is 5.8 km/s.

The variability of the OH maser emission in W33C is best manifested in Stokes parameter V ; therefore, our subsequent analysis is mostly connected with variations of this parameter.

The amplitude of features *1* and *2* observed only in the 1665-MHz line varies very weakly, whereas features *3* and *4* undergo considerable amplitude variations in both main lines (Tables 1 and 2). The listed pairs of features arise owing to splitting of the emission at 33.4 and 39.4 km/s in a longitudinal magnetic field into two components shifted in velocity up and down and elliptically polarized in opposite directions.

In the 1665-MHz line the difference in the radial velocities of features *2* and *1* is 1.7 km/s, and between features *4* and *3* it is 0.8 km/s. A splitting of 1.7 km/s in the emission at 33.4 km/s corresponds to a longitudinal magnetic field of 2.9 mG, and a splitting of 0.8 km/s at 39.4 km/s to 1.4 mG.

In the emission detected by us in the 1667 MHz line, the separation between the Zeeman components *4* and *3* is ≈ 1 km/s (Table 2); this corresponds to a magnetic field of 2.8 mG. The twofold difference in the magnetic field intensity for the emission at 39.4 km/s found from the splitting in the main OH lines can be due to various causes. The emission regions can be close however not coinciding or have different sizes (the region radiating in the 1667-MHz line is more extended). In both cases the medium should be inhomogeneous, turbulent.

The profiles of the 1612- and 1720-MHz OH lines (Fig. 4) consist of emission and absorption components and mirror each other. Such a structure finds its explanation in the model of an OH source that is associated with a molecular cloud around the maser in the presence of an embedded IR emission source affecting the populations of hyperfine-structure sublevels of OH molecules [12]. The particulars of pumping by IR emission in model [12] are such that the inversion in the 1720-MHz transition is accompanied by antiinversion in the 1612-MHz line, and vice versa. Observations of a number of sources in the satellite lines of OH [13, 14] indeed demonstrate mirror profiles of the lines: 1612 MHz in emission, 1720 MHz in absorption, and vice versa. If a magnetic field is present in the cloud, then, according to model [12], inversion or

antiinversion of this or that OH satellite transition is determined by the angle between the direction of propagation of IR emission and the local field vector. With the source inside the cloud, in some parts of it inversion in one of the satellites and antiinversion in the other will be observed; in other parts of the cloud the situation is opposite. If the cloud is not resolved by the radio telescope beam, the superposition of profiles of satellite lines from different parts of the cloud produces a pattern similar to that in Fig. 4.

2.3 Model of the Maser Source in W33C

Let us summarize the results of our OH and H₂O observations. Common for them is that the hydroxyl emission and emission of a group of water-vapor features take place at the same radial velocities (30–40 km/s). Note that the emission in other molecular lines (e.g., CH₃OH [15]) and in radio recombination lines (e.g., H134 α [16]) is also observed in this velocity range. Most likely, these emissions are associated with the same molecular cloud at a radial velocity of about 35 km/s.

We also note that the profiles of the hydroxyl and methanol lines have a double-peaked structure; its components are arranged more or less symmetrically with respect to the velocity 35 km/s. Such a structure of the spectra is best explained by the model of a rotating molecular cloud. The rotation rate is low, i.e., the line-of-sight projection of the cloud rotation rate is small.

The H₂O line profiles have a different structure (Fig. 1 and 2). A sufficiently stable emission at velocities from -7 to 1 km/s and at a velocity of 24 km/s can be associated with the bipolar outflow.

3 MAIN RESULTS

Let us list the main results of our observations of water-vapor and hydroxyl masers in the source W33C.

1. We have detected a large number of strongly variable, short-lived H₂O emission features in a broad interval of radial velocities, from -7 to 55 km/s. The velocity of one of the groups with the most stable emission (34 km/s) is close to the central velocity of the OH absorption line and OH maser emission.

2. We have discovered the maser emission of W33C in the 1667-MHz line in both circular polarizations in the velocity interval 35 – 41 km/s.

3. We have found Zeeman splitting in the OH 1665-MHz main line for the emission at 33.4 and 39.4 km/s. From the splitting magnitude we have estimated the intensity of the line-of-sight component of the magnetic field for each of the regions masering at 33.4 and 39.4 km/s (2.8 and 1.4 mG).

4. “Mirror” profiles of the OH satellite lines, 1612 and 1720 MHz, suggest pumping of the levels of corresponding transitions by IR emission of a source embedded in a magnetized molecular cloud around the maser.

5. We have observed an appreciable variability of the 39.0 - and 39.8 -km/s components of Zeeman splitting in both main lines; at the same time, the 32.6 - and 34.3 -km/s

components in the 1665 MHz line remained rather stable, and in the 1667-MHz line they were not detected at all.

6. The extended spectrum and fast variability of the H₂O maser emission together with the variability of the Zeeman splitting components at 39 km/s in the main OH lines can be a consequence of composite clumpy structure of the molecular cloud and of the presence in it of large-scale (rotation, bipolar outflow) and turbulent motions of material.

ACKNOWLEDGMENTS

This research was supported by the Ministry of Science and Education of the Russian Federation on the facility RT-22 radio telescope (registration number 01-10) and by the Russian Foundation for Basic Research (project code 09-02-00963-a). The authors are grateful to the staff of the Pushchino (Russia) and Nançay (France) radio astronomy observatories for the help with the observations.

References

- [1] M. I. Pashchenko, *Astron. Tsirkulyar* No. 886, 1 (1975).
- [2] M. I. Pashchenko, *Soviet Astron. Lett.* **6**, 58 (1980).
- [3] R. Genzel and D. Downes, *Astron. and Astrophys. Suppl. Ser.* **30**, 145 (1977).
- [4] P. A. Shaver and W. M. Goss, *Austral. J. Phys. Astrophys. Suppl. No. 14*, 77 (1970).
- [5] W. M. Goss and P. A. Shaver, *Austral. J. Phys. Astrophys. Suppl. No. 14*, 1 (1970).
- [6] V. Radhakrishnan, W. M. Goss, J. D. Murray, and J. W. Brooks, *Astrophys. J. Suppl. Ser.* **24**, 49 (1972).
- [7] D. T. Jaffe, R. Güsten, and D. Downes, *Astrophys. J.* **250**, 621 (1981).
- [8] G. Comoretto, F. Palagi, R. Cesaroni, M. Felli, A. Bettarini, M. Catarzi, G. P. Curioni, P. Curioni, S. di Franco, C. Giovanardi, M. Massi, F. Palla, D. Panella, E. Rossi, N. Speroni, and G. Tofani, *Astron. and Astrophys. Suppl. Ser.* **84**, 179 (1990).
- [9] M. I. Pashchenko and E. E. Lekht, *Astron. Reports* **49**, 624 (2005).
- [10] V. I. Slysh, M. I. Pashchenko, G. M. Rudnitskiĭ, V. M. Vitrishchak, and P. Colom, *Astron. Reports* **54**, 599 (2010).
- [11] M. I. Pashchenko, G. M. Rudnitskiĭ, and P. Colom, *Astron. Reports* **53**, 541 (2009).

- [12] V. V. Burdyuzha and D. A. Varshalovich, *Soviet Astron.* **16**, 597 (1973).
- [13] M. I. Pashchenko, G. M. Rudnitskiĭ, and O. Franquelin, *Soviet Astron. Lett.* **5**, 276 (1979).
- [14] R. F. Haynes and J. L. Caswell, *Monthly Not. Roy. Astron. Soc.* **178**, 219 (1977).
- [15] A. D. Haschick, K. M. Menten, and W. A. Baan, *Astrophys. J.* **354**, 556 (1990).
- [16] F. F. Gardner, T. L. Wilson, and P. Thomasson, *Astrophys. Lett.* **16**, 29 (1975).

Table 1: Main components of the V Stokes parameter in the 1665-MHz OH line

Date	F_1 , Jy	F_2 , Jy	$ F_1/F_2 $	$\delta V_{2,1}$, km/s	F_3 , Jy	F_4 , Jy	$ F_3/F_4 $	$\delta V_{4,3}$, km/s
2008.12.05	4.07	-2.07	1.97	1.62	1.4	-1.0	1.4	0.69
2010.04.06	4.30	-2.2	1.95	1.63	2.3	-0.9	2.56	0.80
2010.07.04	3.8	-2.2	1.73	1.67	4.3	-1.4	3.07	0.88
2011.01.07	4.1	-2.3	1.78	1.62	4.3	-2.1	2.05	0.77
2011.05.03	4.3	-2.2	1.95	1.60	3.0	-0.8	3.75	0.81
2011.07.11	4.0	-2.2	1.82	1.62	3.1	-0.9	3.44	0.79

Table 2: Main components of the V Stokes parameter in the 1667-MHz OH line

Date	F_3 , Jy	F_4 , Jy	$ F_3/F_4 $	$\delta V_{4,3}$, km/s
2008.12.05	0.50	-0.85	0.59	1.02
2010.04.06	0.41	-0.76	0.54	0.99
2010.07.04	0.81	-1.38	0.59	1.02
2011.01.07	0.79	-1.15	0.69	0.98
2011.05.03	0.48	-0.57	0.84	1.23
2011.07.11	0.52	-0.53	0.65	0.96

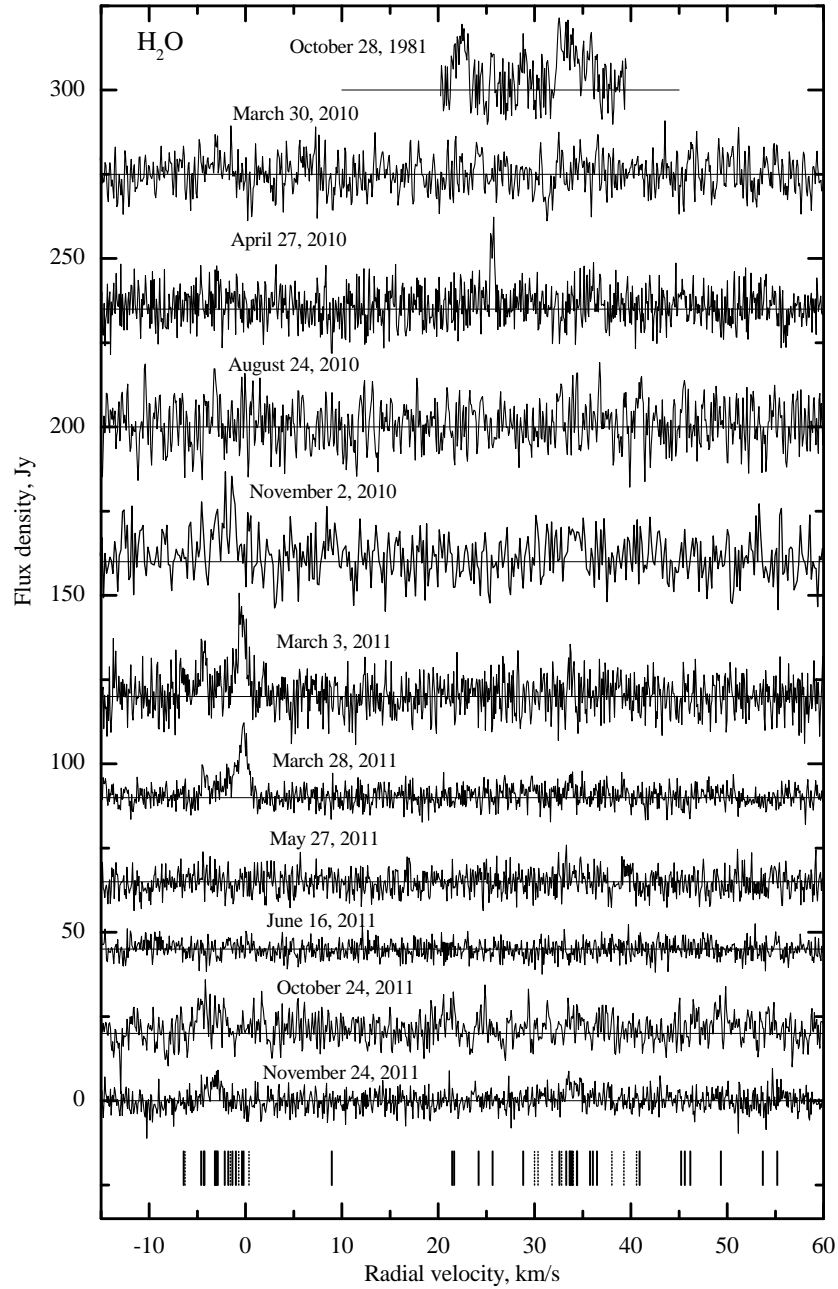


Figure 1: Spectra of the H_2O maser emission toward the source W33C. A double-headed arrow shows the scale. The radial velocity is given with respect to the Local Standard of Rest. Vertical bars at the bottom mark the velocities at which emission features were ever observed by us (solid curves) and other authors (dashed curves).

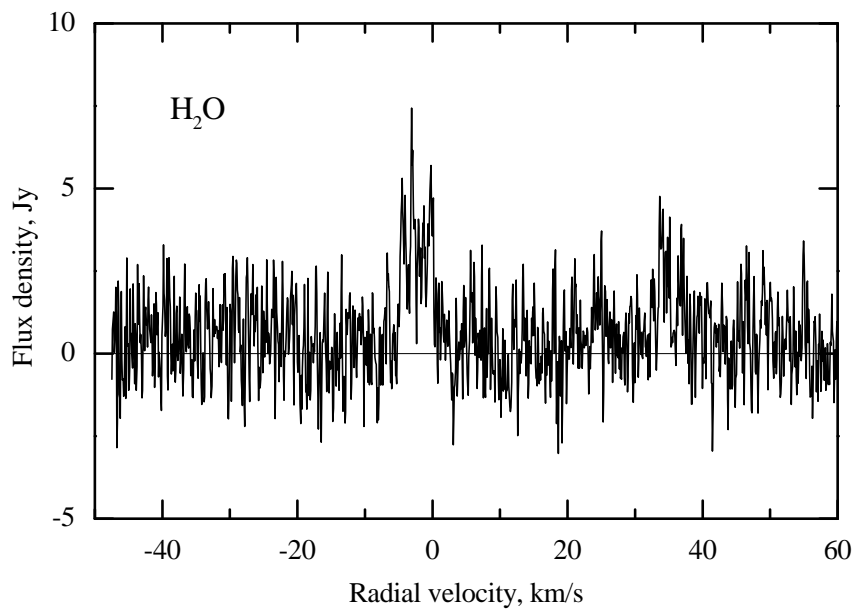


Figure 2: Averaged spectrum of the H₂O maser emission in W33C for a time interval of 2010–2011.

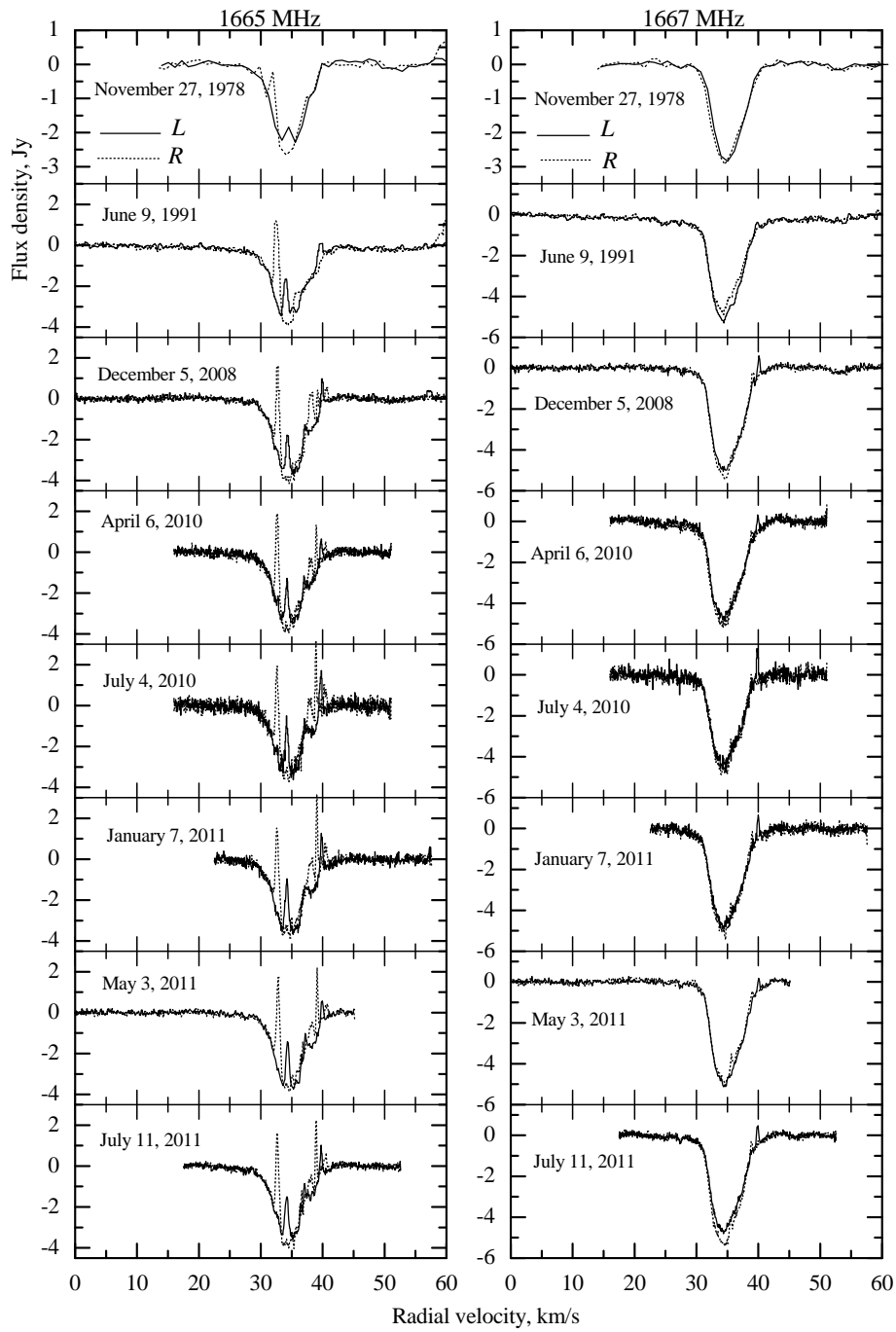


Figure 3: Spectra of maser emission in the 1665- and 1667-MHz hydroxyl lines for left-hand (L) and right-hand (R) circular polarizations at different epochs of the observations.

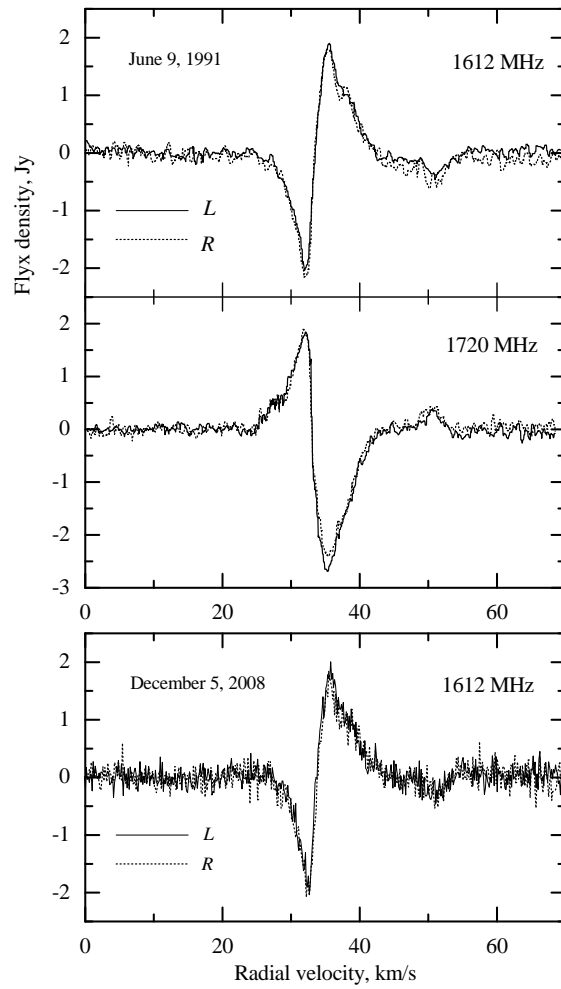


Figure 4: Same as in Fig. 3, but for the 1612 and 1720-MHz satellite lines.

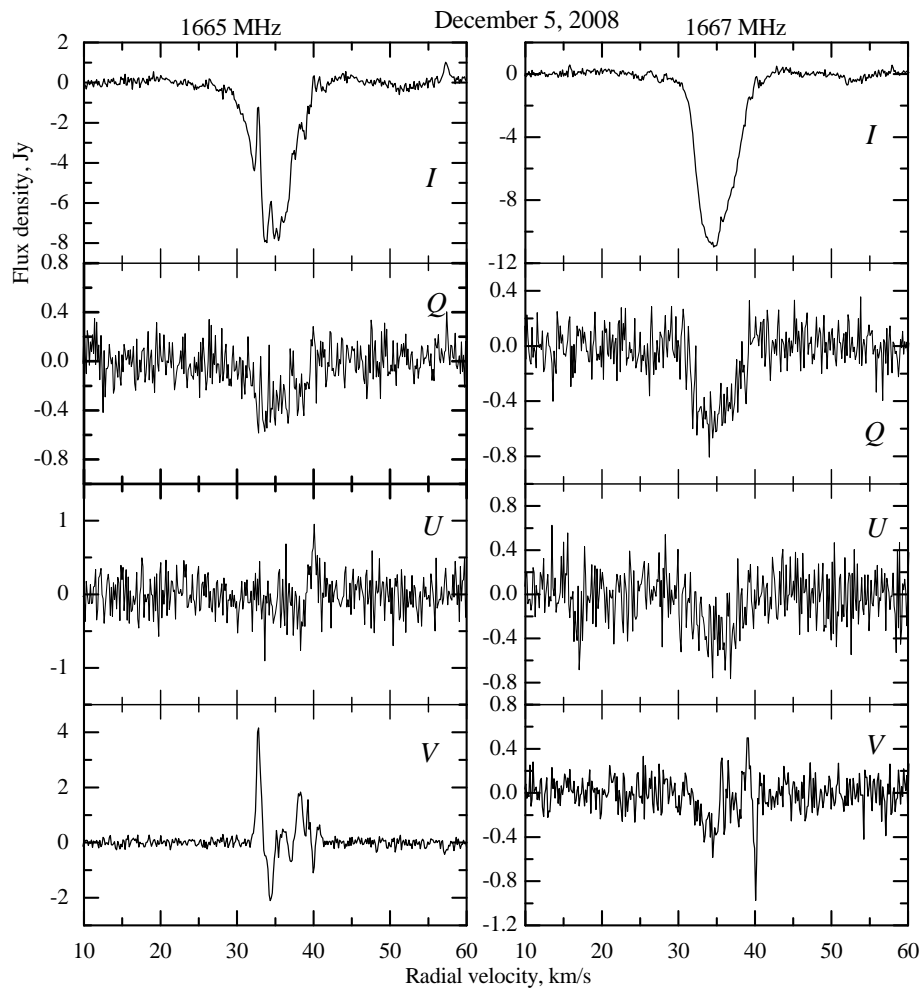


Figure 5: Stokes parameters for the emission in the 1665- and 1667-MHz hydroxyl lines at the epoch of December 5, 2008.

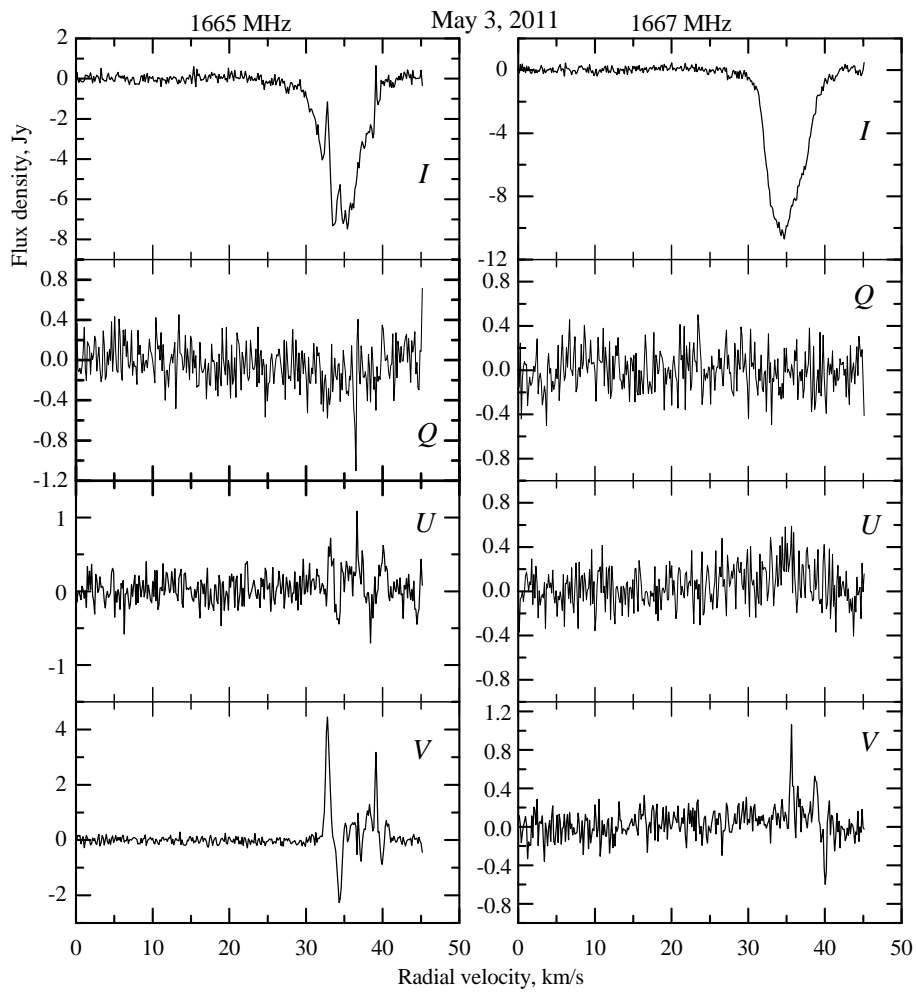


Figure 6: Same as in Fig. 5, but for the epoch of May 3, 2011.

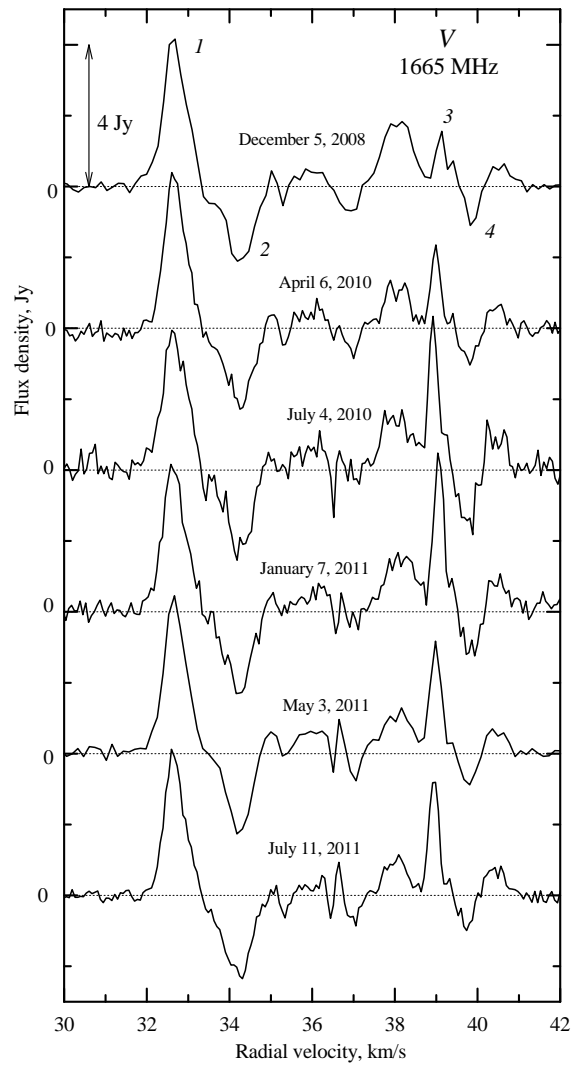


Figure 7: Time variations of Stokes parameter V for the central part of the 1665-MHz spectrum. The main features are numbered.

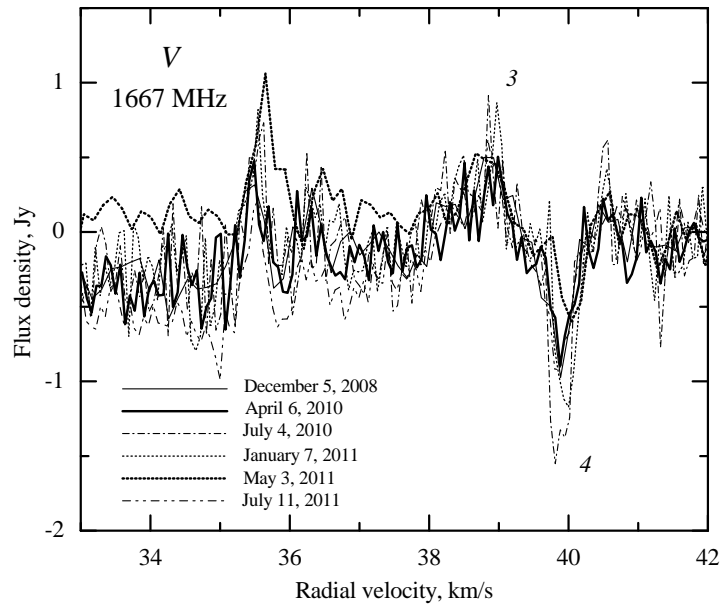


Figure 8: Same as in Fig. 7, but for the central part of the 1667-MHz spectrum.